Torsion instability of soft solid cylinders

Pasquale Ciarletta[*]

*CNRS and Sorbonne Universités, UPMC Univ Paris 06, UMR 7190, Institut Jean le Rond d'Alembert,
4 place Jussieu, case 162, F-75005, Paris, France*
[*]Corresponding author: pasquale.ciarletta@upmc.fr

AND

Michel Destrade

*School of Mathematics, Statistics and Applied Mathematics, National University of
Ireland Galway; University Road, Galway, Ireland*

This article is dedicated to Prof. Ray W. Ogden in friendship and esteem.

The application of pure torsion to a long and thin cylindrical rod is known to provoke a twisting instability, evolving from an initial kink to a knot. In the torsional parallel-plate rheometry of stubby cylinders, the geometrical constraints impose zero displacement of the axis of the cylinder, preventing the occurrence of such twisting instability. Under these experimental conditions, wrinkles occur on the cylinder's surface at a given critical angle of torsion. Here we investigate this subclass of elastic instability—which we call *torsion instability*—of soft cylinders subject to a combined finite axial stretch and torsion, by applying the theory of incremental elastic deformation superimposed on finite strains. We formulate the incremental boundary elastic problem in the Stroh differential form, and use the surface impedance method to build a robust numerical procedure for deriving the marginal stability curves. We present the results for a Mooney–Rivlin material and study the influence of the material parameters on the elastic bifurcation.

Keywords: elastic stability; torsion; Stroh formulation; surface impedance; central-impedance matrix

1. Introduction

The application of combined finite axial stretch and finite torsion to a solid right cylinder constitutes one of the few universal solutions of nonlinear isotropic incompressible elasticity, where here 'universal' means that the deformation can be achieved for any homogeneous hyperelastic material by the application of surface tractions alone.

The simple torsion of a solid cylinder can be defined as the deformation by which planes perpendicular to the axis of the cylinder are rotated in their own plane through an angle proportional to their distance from one end surface. In a seminal paper, Rivlin (1948a) found that a state of simple torsion can be maintained by surface tractions alone (end couples and end compressive normal forces) for any incompressible, neo-Hookean material. Further extensions were made in subsequent papers of the same series by Rivlin, who calculated analytical expressions of such surface tractions for a generic incompressible, isotropic material (Rivlin, 1948b), and for a hyperelastic tube subjected to combined axial stretching and torsion (Rivlin, 1949). In that latter paper, Rivlin mentions that Dr H.A. Daynes had drawn his attention to the earlier work of Poynting (1909), who had observed and measured the lengthening of a steel wire and of a rubber rod upon twisting, and Rivlin provided a satisfactory theoretical
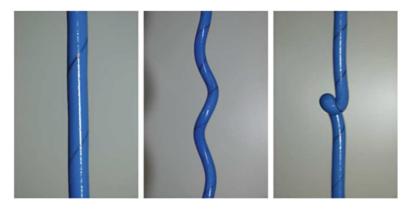
Fig. 1. Twisting a long cylindrical rod made of polyurethane: at first a large torsion takes place, followed by 'twisting instability' allowing for displacements on the axis, eventually turning into a twisting knot.

explanation to this phenomenon, later referred to as the *positive Poynting effect*. The results of Rivlin were revisited and extended by many over the years. For instance, Horgan & Saccomandi (1999) found that, if the strain energy density function used to model the behaviour of the cylinder depended only on the first principal strain invariant, then there must exist a universal relation between the surface force and the torque (universal relative to the class of incompressible materials with strain energy depending only on the first principal invariant). Such a relative-universal relation is unlikely to be observed in practice, indicating that the strain energy should also depend on the second invariant. Additional discussion on this subject was later provided by Wineman (2005).

It is intuitive to expect that the application of a compressive axial force during simple torsion should eventually lead to a buckling instability once a certain threshold of torsion rate is reached. However, there are very few studies of *torsional instabilities* on a solid cylinder to be found in the literature. Green & Spencer (1959) found an analytical solution for neo-Hookean solids in the subclass of instability modes giving rise to finite displacements on the axis of the cylinder. Duka *et al.* (1993) later studied the numerical solution of this instability subclass for a generic Mooney–Rivlin solid. As initially guessed by Green & Spencer (1959), their solution represents the 'twisting instability' of a cylindrical rod, evolving from an initial kink to a knot, see Fig. 1, and Gent & Hua (2004) later presented an energetic analysis of this transition.

A recent experiment by Mora *et al.* (2011) shows that when a cylindrical sample of soft gel with small axial length/external radius ratio is deformed by a rheometer, it eventually displays a wrinkling instability pattern on its surface at a finite critical value of the torsion rate, see their Fig. 4. In that experimental scenario, the possibility of a displacement on the axis of the cylinder is prevented by the geometrical constraints, and so an instability other than twisting is observed. This particular effect can be easily reproduced by applying a torque by hand on a soft, short cylinder, as reproduced in Fig. 2. The aim of our work is to investigate the onset of this new subclass of wrinkling instabilities for an isotropic, incompressible, hyperelastic material. We call them *torsion instabilities*.

The paper is organized as follows. In Section 2, we recall the equations governing the kinematics of the finite axial stretching and torsion of the soft cylinder, and derive the axial-symmetric solution. We specialize the analysis to the class of Mooney–Rivlin materials in order to keep the number of constitutive parameters low, while retaining dependence of the strain energy density on the first two principal
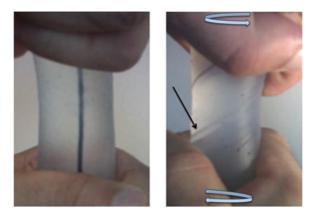
FIG. 2. A short cylinder made of silicone rubber at rest (left) and after applying by hand a torque at the end surfaces (right). We marked a solid black line to follow the deformation on the cylinder, while the arrow indicates the wrinkles formed at a critical torsion rate.

strain invariants. In Section 3, we perform an incremental (linearized) stability analysis, by superposing a small-amplitude perturbation on this basic finite deformation. The incremental boundary-value problem is derived and the corresponding numerical results are presented in Section 4 and discussed in Section 5.

2. Finite torsion and stretching of a soft elastic cylinder

Let us consider an elastic cylinder made of an isotropic, homogeneous, nonlinearly elastic, incompressible material, with axial length L and external radius R_o in the fixed reference configuration Ω_0. Using cylindrical coordinate systems, the kinematics of the deformation can be defined by a mapping $\chi: \Omega_0 \to \Re^3$ that brings the material point $\mathbf{X} = \mathbf{X}(R, \Theta, Z)$ to the spatial position $\mathbf{x} = \mathbf{x}(r, \theta, z) = \chi(\mathbf{X})$ in the deformed configuration, where (R, Θ, Z) and (r, θ, z) are the coordinates along the orthonormal vector bases $(\mathbf{E_1}, \mathbf{E_2}, \mathbf{E_3})$ and $(\mathbf{e_1}, \mathbf{e_2}, \mathbf{e_3})$, respectively. In particular, the soft cylinder is subjected to a finite stretching and torsion, so that:

$$r = \frac{R}{\sqrt{\lambda_z}}, \quad \theta = \Theta + \gamma \lambda_z Z, \quad z = \lambda_z Z, \tag{2.1}$$

where γ is the torsion angle per unit length and λ_z is the uniform stretching ratio in the axial direction ($\gamma \lambda_z L$ is the angle of torsion of the whole cylinder). In the current deformation, the cylinder has radius $r_o = R_o/\sqrt{\lambda_z}$ and length $l = \lambda_z L$.

From Equation (2.1), the deformation gradient $\mathbf{F} = \partial \chi / \partial \mathbf{X}$ has the following components in the $\mathbf{e_i} \otimes \mathbf{E_j}$ basis,

$$\mathbf{F} = \begin{bmatrix} \dfrac{1}{\sqrt{\lambda_z}} & 0 & 0 \\ 0 & \dfrac{1}{\sqrt{\lambda_z}} & r\gamma\lambda_z \\ 0 & 0 & \lambda_z \end{bmatrix}, \tag{2.2}$$

and clearly, $\det \mathbf{F} = 1$, so that the imposed deformation is volume preserving and compatible with the constraint of incompressibility.

From a constitutive viewpoint, we assume from now on that the cylinder behaves as a *Mooney–Rivlin hyperelastic material*, so that its strain energy density W is given by

$$W = \frac{c_1}{2}(I_1 - 3) + \frac{c_2}{2}(I_2 - 3), \tag{2.3}$$

where c_1, c_2 are positive material constants (and $\mu = c_1 + c_2$ is the shear modulus) and I_1, I_2 are the first two principal invariants of the left Cauchy–Green deformation tensor $\mathbf{b} = \mathbf{F}\mathbf{F}^\top$, where the superscript $\top$ denotes the transpose. Note that not all generality is lost by specializing the strain energy so early. In particular, the Mooney–Rivlin strain energy function encompasses all weakly nonlinear elastic incompressible models up to the third-order in the strain, as shown by Rivlin & Saunders (1951) (see Destrade *et al.*, 2010 for another proof). Also, as long as $c_2 \neq 0$, the problem of a relative-universal relation, unlikely to be observed in practice, is avoided (more on this later).

From (2.2), we find the components of $\mathbf{b}$ in the $\mathbf{e_i} \otimes \mathbf{e_j}$ basis as

$$\mathbf{b} = \begin{bmatrix} \lambda_z^{-1} & 0 & 0 \\ 0 & \lambda_z^{-1} + \gamma^2 r^2 \lambda_z^2 & r\gamma \lambda_z^2 \\ 0 & r\gamma \lambda_z^2 & \lambda_z^2 \end{bmatrix}, \tag{2.4}$$

and thus compute its principal invariants as

$$I_1 = \operatorname{tr} \mathbf{b} = \lambda_z^2 + 2\lambda_z^{-1} + \gamma^2 r^2 \lambda_z^2, \quad I_2 = \tfrac{1}{2}[\operatorname{tr}(\mathbf{b}^2) - \operatorname{tr}^2 \mathbf{b}] = 2\lambda_z + \lambda_z^{-2} + \gamma^2 r^2 \lambda_z^2. \tag{2.5}$$

Using the constitutive relation in Equation (2.3), the Cauchy stress tensor $\boldsymbol{\sigma}$ can be written, by Rivlin's representation theorem, as

$$\boldsymbol{\sigma} = c_1 \mathbf{b} - c_2 \mathbf{b}^{-1} - p\mathbf{I}, \tag{2.6}$$

where $\mathbf{I}$ is the second-order identity tensor, and p is a Lagrange multiplier arising from the incompressibility constraint $(\det \mathbf{F} - 1) = 0$, to be determined from the equations of equilibrium and the boundary conditions. Here, the non-zero components of the Cauchy stress from Equation (2.6) read

$$\begin{aligned} \sigma_{rr} &= c_1 \lambda_z^{-1} - c_2 \lambda_z - p, \\ \sigma_{\theta\theta} &= c_1(\lambda_z^{-1} + \gamma^2 r^2 \lambda_z^2) - c_2 \lambda_z - p, \\ \sigma_{zz} &= c_1 \lambda_z^2 - c_2(\lambda_z^{-2} + \gamma^2 r^2 \lambda_z) - p, \\ \sigma_{\theta z} &= \sigma_{z\theta} = c_1 \gamma r \lambda_z^2 - c_2 \gamma r \lambda_z, \end{aligned} \tag{2.7}$$

and, in the absence of body forces, the equilibrium equations are

$$\operatorname{div} \boldsymbol{\sigma} = \mathbf{0}. \tag{2.8}$$

For the axis-symmetric deformation fields in Equation (2.1), the only non-vanishing equilibrium equation in Equation (2.8) is

$$\frac{\partial(r\sigma_{rr})}{\partial r} - \sigma_{\theta\theta} = 0, \tag{2.9}$$

and the traction-free boundary conditions at the external radius are

$$\sigma_{rr}(r_o) = 0 \quad \text{at } r_o = R_0/\sqrt{\lambda_z}. \tag{2.10}$$

By integrating σ_{rr} in Equation (2.9), subject to Equation (2.10), the Lagrange multiplier p can be determined as

$$p = \frac{c_1}{\lambda_z} - c_2\lambda_z + \int_r^{r_o} c_1 r\gamma^2\lambda_z^2 \, dr = c_1\left[\frac{1}{\lambda_z} + \frac{\gamma^2\lambda_z^2}{2}(r_o^2 - r^2)\right] - c_2\lambda_z. \tag{2.11}$$

Finally, it is straightforward to show that such a finite torsion and stretching of the cylinder can be obtained by applying the following normal force N and a torque M on the end surfaces,

$$N = 2\pi \int_{r=0}^{r_o} \sigma_{zz} r \, dr = \pi R_o^2 \left[(\lambda_z - \lambda_z^{-2})(c_1 + c_2\lambda_z^{-1}) - \frac{\gamma^2 R_o^2}{2}(c_1 + 2c_2\lambda_z^{-1})\right] \tag{2.12}$$

and

$$M = 2\pi \int_{r=0}^{r_o} \sigma_{z\theta} r^2 \, dr = \frac{\pi\gamma R_o^4}{2}(c_1 + c_2\lambda_z^{-1}), \tag{2.13}$$

where Equations (2.7) and (2.11) have been used, see Rivlin & Saunders (1951).

In *simple torsion*, there is no axial stretch: $\lambda_z = 1$, and those expressions simplify to

$$N = -\frac{\pi\gamma^2 R_o^4}{4}(c_1 + 2c_2), \quad M = \frac{\pi\gamma R_o^4}{2}(c_1 + c_2). \tag{2.14}$$

Here we first note that an axial compression is needed for imposing simple torsion because $N < 0$. This is the so-called *positive Poynting effect* for hyperelastic solids, which is a nonlinear elastic effect forcing the spread of the top surfaces of a cylinder under torsion. This axial compression increases quadratically with an increasing torsional strain, and it is reasonable to hypothesize that a buckling instability may occur beyond a certain critical torsion. We investigate this possibility in the next section. Second, we note that if the dependence on I_2 was dropped by taking $c_2 = 0$ above (neo-Hookean case), then the following relative-universal relation would be in force: $2N/\gamma^2 = -M/\gamma$. In their experiments on a vulcanized rubber cylinder of length and radius $L = R_o = 2.5$ cm, Rivlin & Saunders (1951) found indeed that N and M were proportional to γ^2 and γ, respectively, in agreement with Equation (2.14). However, they found that $2N/\gamma^2 = -0.0212\,\text{N/m}^2$ and $M/\gamma = 0.0157\,\text{N/m}^2$ (Drozdov, 1996), showing that the relative-universal relation does not hold and that the rubber in question must be modelled as a Mooney–Rivlin material, not as neo-Hookean.

3. Linear stability analysis

In this section, we perform a linear stability analysis of the axis-symmetric solution for a soft cylinder subjected to finite torsion and stretching. For this purpose, we first introduce the theory of incremental deformations superimposed on finite strains. Next, we derive the incremental equilibrium equations and boundary conditions in the Stroh form and finally, we propose a robust numerical procedure for solving the resulting boundary value problem.

3.1 *Incremental elastic theory*

We perform a perturbation of the large axis-symmetric solution given by Equations (2.1), (2.7) and (2.11) by using the theory of incremental deformations superimposed on finite strains (Ogden, 1997). In practice, we proceed by writing

$$\mathbf{x}_p = \boldsymbol{\chi}(\mathbf{X}) + \dot{\boldsymbol{\chi}}(\mathbf{x}), \tag{3.1}$$

where $\mathbf{x}_p$ is the perturbed spatial position, and we assume that the incremental displacement $\dot{\boldsymbol{\chi}}$ is infinitesimal and represents a first-order correction.

We define the associated spatial displacement gradient as $\boldsymbol{\Gamma} = \text{grad}\,\dot{\boldsymbol{\chi}}$, and by simple differentiation rules we find that the perturbed deformation gradient $\mathbf{F}_p$ reads

$$\mathbf{F}_p = \mathbf{F} + \dot{\mathbf{F}} = \mathbf{F} + \boldsymbol{\Gamma}\mathbf{F}, \tag{3.2}$$

where $\dot{\mathbf{F}}$ is the incremental deformation gradient. Performing a series expansion of the constitutive relation in Equation (2.6) to the first order, we express the components of the incremental stress $\dot{\mathbf{S}}$, i.e. the push-forward of the nominal stress, as

$$\dot{S}_{ji} = L_{jikl}\Gamma_{kl} + p\Gamma_{ji} - \dot{p}\delta_{ji}, \tag{3.3}$$

where $\dot{p}$ is the increment in the Lagrange multiplier p, δ_{ji} is the Kronecker delta, and L_{jikl} are the components of the fourth-order tensor of instantaneous moduli, i.e. the push-forward of the fixed reference elasticity tensor. Explicitly,

$$L_{jikl} = F_{j\gamma}F_{k\beta}\frac{\partial^2 W}{\partial F_{i\gamma}\,\partial F_{l\beta}}, \tag{3.4}$$

where Einstein's summation rule on repeated indices is assumed. For instance, the moduli for the Mooney–Rivlin material (2.3) are

$$L_{jilk} = c_1 b_{jl}\delta_{ik} + c_2[2b_{ij}b_{kl} + (b_{nn}b_{jk} - (\mathbf{b}^2)_{jk})\delta_{il} - b_{il}b_{jk} - b_{ik}b_{jl}]. \tag{3.5}$$

Now, the incremental equilibrium equations take the following form:

$$\text{div}\,\dot{\mathbf{S}} = \mathbf{0}, \tag{3.6}$$

while the vanishing of the incremental traction at the free surface gives

$$\dot{S}_{rr} = \dot{S}_{r\theta} = \dot{S}_{rz} = 0 \quad \text{at } r_o = R_0/\sqrt{\lambda_z}. \tag{3.7}$$

Finally, the incremental incompressibility constraint is written as

$$\text{tr}\,\boldsymbol{\Gamma} = 0. \tag{3.8}$$

Equations (3.6–3.8) represent the incremental boundary value problem, whose solution is now investigated.
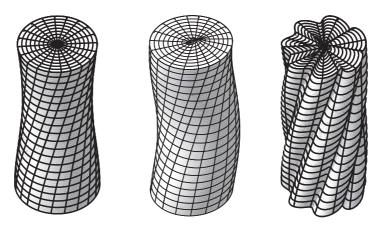
FIG. 3. Surface pattern generated by a torsion instability perturbation superimposed on the finite torsion of a right cylinder. Here we implement a perturbation in the form of a torsion instability where for illustrative purposes we take the angle of torsion to be 60°, no axial pre-stretch, and the amplitude of the perturbation to be one-tenth of the current radius. We chose to have one wavelength axially (all three pictures) and, in turn, a circumferential wave number $m = 0$ (left), $m = 1$ (middle) and $m = 7$ (right).

3.2 *Stroh formulation of the incremental problem*

We develop the incremental deformation fields $\chi = [u_r, u_\theta, u_z]^\top$ by separation of variables, in the following form:

$$u_r(r, \theta, z) = U(r) \cos(m\theta - k_z z), \quad [u_\theta(r, \theta, z), u_z(r, \theta, z)]^\top = [V(r), W(r)]^\top \sin(m\theta - k_z z), \quad (3.9)$$

where U, V are W are functions of r only, the *circumferential mode number m* is an integer, and the *axial wavenumber k_z* is a real number.

Figure 3 displays different modes that can be expressed by such a perturbation. For illustrative purposes there, we took a right cylinder of stubbiness $L/r_o = 5$, subject to a large torsion of angle $\gamma L = 60°$ and no axial pre-stretch ($\lambda_z = 1$), onto which we superimposed a perturbation in the form of Equation (3.9), with $U(r_o) = V(r_o) = W(r_o) = 0.1r_o$ (small amplitude perturbation) and $k_z r_o = 1$ (axial wave number). (For a more accurate picture of an actual torsion instability, the critical parameters γ, k_z, and the relative displacements $U(r_o)$, $V(r_o)$ and $W(r_o)$, must be computed from the stability analysis of Section 4, depending on the values of the constitutive parameters c_1 and c_2.) By observation of Equation (3.9) and of the figure we can confirm that from now on we can discard the case $m = 0$ because it represents an axis-symmetric perturbation, of no relevance to torsional instability. We further note that the pictures for the $m = 0$ and $m = 1$ perturbation modes closely match those of the early Euler buckling of a right cylinder under compression, see De Pascalis *et al.* (2011).

We now try to model the experimental conditions at play in the torsion and stretch deformation field created by a rheometer. Because there, the top and bottom faces are glued to plates rotating about a fixed axis, we impose that the centre of the top face be directly aligned with that of the bottom face. This is achieved when

$$k_z = \frac{2n\pi}{l} = \frac{2n\pi}{\lambda_z L}, \qquad (3.10)$$

where the integer n is the *axial mode number*.

By substituting Equation (3.9) into Equation (3.3), we can express the components of the incremental stress tensor in a form similar to that of the displacements,

$$
\begin{aligned}
{[\dot{S}_{rr}(r,\theta,z), \dot{p}(r,\theta,z)]}^{\top} &= [S_{rr}(r), P(r)]^{\top} \cos(m\theta - k_z z), \\
{[\dot{S}_{r\theta}(r,\theta,z), \dot{S}_{rz}(r,\theta,z)]}^{\top} &= [S_{r\theta}(r), S_{rz}(r)]^{\top} \sin(m\theta - k_z z),
\end{aligned}
\tag{3.11}
$$

say, where P and S_{ij} are functions of r only.

This formulation allows a great simplification of the boundary value problem. Hence, the incompressibility constraint in Equation (3.8) can be rewritten as

$$
U + mV + r(U' - k_z W) = 0,
\tag{3.12}
$$

where the prime denotes differentiation with respect to r. Moreover, the increment $\dot{p}$ of the Lagrange multiplier can be found from the constitutive equation for $\dot{s}_{rr}$, as follows:

$$
P = -rS_{rr} + L_{rr\theta\theta}(U + mV) - k_z r L_{rrz\theta}V + m L_{rr\theta z}W - k_z r L_{rrzz}W + r(p + L_{rrrr})U'.
\tag{3.13}
$$

Further simplifications arise once we introduce the *displacement-traction vector* $\boldsymbol{\eta}$ as

$$
\boldsymbol{\eta} = [U, V, W, irS_{rr}, irS_{r\theta}, irS_{rz}]^{\top},
\tag{3.14}
$$

where 'i' is the imaginary unit. Indeed, using Equations (3.9), (3.11) and (3.13), it is possible to rewrite the entire boundary value problem given by Equations (3.3), (3.6) and (3.8) as the following first-order differential system:

$$
\frac{d\boldsymbol{\eta}}{dr} = \frac{i}{r}\mathbf{G}\boldsymbol{\eta},
\tag{3.15}
$$

which is called the *Stroh formulation* of the incremental problem. In particular, the Stroh matrix $\mathbf{G}$ admits the following block representation:

$$
\mathbf{G} = \begin{bmatrix} \mathbf{G}_1 & \mathbf{G}_2 \\ \mathbf{G}_3 & \mathbf{G}_1^+ \end{bmatrix},
\tag{3.16}
$$

where the 3×3 sub-blocks $\mathbf{G}_2$ and $\mathbf{G}_3$ are real symmetric, and the symbol $+$ denotes the adjugate (i.e. transpose conjugate) matrix operator. In particular, the matrices $\mathbf{G}_1$ and $\mathbf{G}_2$ admit the following simplified representations:

$$
\mathbf{G}_1 = \begin{bmatrix} i & im & -ik_z r \\ \dfrac{i\delta_1}{\beta} & -\dfrac{i\delta_2}{\beta} & 0 \\ -\dfrac{i\delta_3}{\beta} & -\dfrac{i\delta_4}{\beta} & 0 \end{bmatrix}, \quad \mathbf{G}_2 = \begin{bmatrix} 0 & 0 & 0 \\ 0 & \dfrac{L_{rzrz}}{\beta} & -\dfrac{L_{r\theta rz}}{\beta} \\ 0 & -\dfrac{L_{r\theta rz}}{\beta} & \dfrac{L_{rzrz}}{\beta} \end{bmatrix},
\tag{3.17}
$$

with

$$\beta = L_{r\theta rz}^2 - L_{r\theta r\theta}L_{rzrz},$$

$$\delta_1 = m[(p + L_{r\theta\theta r})L_{rzzr} - L_{r\theta rz}L_{rz\theta r}] + k_z r[-L_{r\theta zr}L_{rzrz} + L_{r\theta rz}(p + L_{rzzr})],$$

$$\delta_2 = -(p + L_{r\theta\theta r})L_{rzrz} + L_{r\theta rz}L_{rz\theta r},$$

$$\delta_3 = m[(p + L_{r\theta e\theta})L_{rzr\theta} - L_{r\theta r\theta}L_{rzr\theta}] + k_z r[-L_{r\theta zr}L_{r\theta rz} + L_{r\theta r\theta}(p + L_{rzzr})],$$

$$\delta_4 = (p + L_{r\theta r\theta})L_{rzr\theta} - L_{r\theta r\theta}L_{rz\theta r}. \tag{3.18}$$

The expression of $\mathbf{G}_3$ is very lengthy and although we have obtained it formally with a Computer Algebra System, we do not report it here for the sake of brevity. Great simplifications arise when dealing with a neo-Hookean material ($c_1 = \mu$, $c_2 = 0$), as reported in Appendix.

Finally, considering that m and k_z are integer- and real-valued, respectively, it is easy to show that the Stroh matrix $\mathbf{G}$ displays the following symmetry (Shuvalov, 2003):

$$\mathbf{G} = \mathbf{T}\mathbf{G}^+\mathbf{T}, \tag{3.19}$$

where $\mathbf{T}$ has zero diagonal sub-block matrices, while off-diagonal blocks are identity matrices.

The Hamiltonian structure and algebraic properties of the Stroh matrix form the basis of the robust asymptotic and numerical procedures presented in the next sections. We note that Duka *et al.* (1993) have also put the incremental problem in the form of a first-order differential system, although not in the present, optimal, Stroh form.

3.3 *Numerical solution using the solid-cylinder impedance matrix*

Following Shuvalov (2003), we rely on the *impedance matrix method* for solving the incremental elastic problem.

Let us define the 6×6 matricant $\mathbf{M}(r, r_i)$ as the solution of the initial value problem:

$$\left[\frac{\mathrm{d}}{\mathrm{d}r} - \frac{\mathrm{i}}{r}\mathbf{G}(r)\right]\mathbf{M}(r, r_i) = \mathbf{0} \quad \text{with } \mathbf{M}(r_i, r_i) = \mathbf{I}_{(6)}, \quad r, r_i \neq 0. \tag{3.20}$$

Thus, from Equations (3.15, 3.20), the displacement-traction vector solution can be expressed as follows:

$$\boldsymbol{\eta}(r) = \mathbf{M}(r, r_i)\boldsymbol{\eta}(r_i) = \begin{bmatrix} \mathbf{M}_1(r, r_i) & \mathbf{M}_2(r, r_i) \\ \mathbf{M}_3(r, r_i) & \mathbf{M}_4(r, r_i) \end{bmatrix} \boldsymbol{\eta}(r_i). \tag{3.21}$$

Now if we define

$$\mathbf{u} = [U(r), V(r), W(r)]^\top, \quad \mathbf{t} = [S_{rr}(r), S_{r\theta}(r), S_{rz}(r)]^\top, \tag{3.22}$$

as the displacement and traction vectors, respectively, then the displacement-traction vector can be expressed as $\boldsymbol{\eta} = [\mathbf{u}, \mathrm{i}r\,\mathbf{t}]^\top$. It is then possible to define a functional relation between the traction and the displacements vectors, reading:

$$r\mathbf{t} = \mathbf{Z}\mathbf{u}, \tag{3.23}$$

where $\mathbf{Z}$ is a *surface impedance matrix*. Here, one can build an expression for $\mathbf{Z}$ either by using the *conditional* (i.e depending on its value at $r = r_i$) impedance matrix, as $\mathbf{Z} = \mathbf{Z}(r, r_i) = -\mathrm{i}\mathbf{M}_3(r, r_i)\mathbf{M}_1^{-1}(r, r_i)$ for a stress-free boundary condition imposing $\mathbf{Z}(r_i) = 0$, or by using the *solid-cylinder impedance matrix*

$\mathbf{Z} = \mathbf{Z}(r)$, independent of an auxiliary condition at some other coordinate, see Shuvalov & Norris (2010) for details.

In either way, the Stroh formulation in Equation (3.15) can be manipulated by substituting Equation (3.23) to eliminate the dependence on $\mathbf{u}$. Accordingly, the differential system is transformed into a *differential Riccati equation* for $\mathbf{Z}$, namely

$$\frac{\mathrm{d}}{\mathrm{d}r}\mathbf{Z} = \frac{1}{r}\left(\mathbf{G}_3 + \mathbf{Z}\mathbf{G}_2\mathbf{Z} - \mathrm{i}\mathbf{Z}\mathbf{G}_1 + \mathrm{i}\mathbf{G}_1^+\mathbf{Z}\right). \tag{3.24}$$

Recalling, from Equation (2.13), that the matricant solution diverges for $r \to 0$, this method is of no use for determining the solution on the cylinder axis. Conversely, the limiting value $\mathbf{Z}_0 \equiv \mathbf{Z}(r = 0)$ in Equation (3.23), also known as *central-impedance matrix* (Shuvalov & Norris, 2010), is of utmost importance for solving the incremental problem of a solid cylinder. Shuvalov (2003) demonstrated that the fundamental solution of Equation (3.15), having a regular singular point at $r = 0$, can be expressed in the form of a Frobenius series depending on the eigenspectrum of the matrix $\mathrm{i}\mathbf{G}(0)$. From Equations (2.2), (3.4), (3.16) and (3.17), we find that the sub-blocks of $\mathbf{G}(0)$ read:

$$\mathbf{G}_1(0) = \begin{bmatrix} \mathrm{i} & \mathrm{i}m & 0 \\ \bar{\delta} & \bar{\delta} & 0 \\ 0 & 0 & 0 \end{bmatrix},$$

$$\mathbf{G}_2(0) = \begin{bmatrix} 0 & 0 & 0 \\ 0 & -\dfrac{\lambda_z(c_1\lambda_z + c_2)}{c_1^2\lambda_z + c_1 c_2\left(1 + \lambda_z^3\right) + c_2^2\lambda_z^2} & 0 \\ 0 & 0 & -\dfrac{\lambda_z(c_1\lambda_z + c_2)}{c_1^2\lambda_z + c_1 c_2\left(1 + \lambda_z^3\right) + c_2^2\lambda_z^2} \end{bmatrix} \tag{3.25}$$

with

$$\bar{\delta} = \mathrm{i}\frac{2c_2^2(1 + \lambda_z^3) + c_2\lambda_z^3(-\gamma^2 R_o^2 + 2\lambda_z)c_1 + \lambda_z^2(-2 - \gamma^2 R_o^2\lambda_z^2)c_1^2}{2\lambda_z(c_2^2\lambda_z^2 + c_2(1 + \lambda_z^3)c_1 + \lambda_z c_1^2)},$$

and

$$\mathbf{G}_3(0) = \begin{bmatrix} -\dfrac{\mathrm{i}(-16 - 4\gamma^2(R_o^2 - m^2 R_o^2)\lambda_z^2 + \gamma^4 m^2 R_o^4\lambda_z^4)}{4\lambda_z} & -\dfrac{\mathrm{i}m(-16 + \gamma^4 R_o^4\lambda_z^4)}{4\lambda_z} & 0 \\ -\dfrac{\mathrm{i}m(-16 + \gamma^4 R_o^4\lambda_z^4)}{4\lambda_z} & \dfrac{\mathrm{i}(4\,m^2(4 + \gamma^2 R_o^2\lambda_z^2) + \lambda_z^2(-4\gamma^2 R_o^2 - \gamma^4 R_o^4\lambda_z^2))}{4\lambda_z} & 0 \\ 0 & 0 & \dfrac{\mathrm{i}m^2}{\lambda_z} \end{bmatrix} \tag{3.26}$$

Using Equations (3.25) and (3.26), it is now possible to show that the eigenvalues of $\mathrm{i}\mathbf{G}(0)$ are $\lambda_G = \{\pm(m-1), \pm m, \pm(m+1)\}$, all independent on the imposed deformation and on the material properties. In particular, we find that all such eigenvalues λ_G differ by an integer, so that the Frobenius power expansion requires the introduction of additional terms compared to the solution given by Shuvalov & Norris (2010). Moreover, in the case $m = 1$ we also find that $\mathrm{i}\mathbf{G}(0)$ is not semi-simple, due to the presence of rigid-body motions. We discuss this special case in further detail in the next section.

For our purposes, it is easier to identify the central impedance matrix $\mathbf{Z}_0$ as the stable solution of the following algebraic Riccati equation (Shuvalov & Norris, 2010),

$$\mathbf{G}_3(0) + \mathbf{Z}_0\mathbf{G}_2(0)\mathbf{Z}_0 - i\mathbf{Z}_0\mathbf{G}_1(0) + i\mathbf{G}_1^+(0)\mathbf{Z}_0 = \mathbf{0}, \tag{3.27}$$

hence avoiding non-physical singularity at $r = 0$ in Equation (3.24). The stable solution is the unique, symmetric, semi-definite solution $\mathbf{Z}_0$ which can be found by imposing that all eigenvalues of the matrix $-i\mathbf{G}_1(0) + \mathbf{G}_2(0)\mathbf{Z}_0$ be negative. Considering the Taylor expansion $\mathbf{Z}(r) = \sum_{n=0}^{\infty} \mathbf{Z}_n r^n$, the matrix $\mathbf{Z}_1$ can be calculated from Equation (3.24) at the first order in r, as the stable solution of the following algebraic Riccati equation:

$$\mathbf{G}_3(r) + \mathbf{Z}_0\mathbf{G}_2(r)\mathbf{Z}_0 - i\mathbf{Z}_0\mathbf{G}_1(r) + i\mathbf{G}_1^+(r)\mathbf{Z}_0 + r^2\mathbf{Z}_1\mathbf{G}_2(r)\mathbf{Z}_1$$
$$- ir\mathbf{Z}_1\left[\mathbf{G}_1(r) - \mathbf{G}_2(r)\mathbf{Z}_0 - \frac{i}{2}\mathbf{I}\right] + ir\left[\mathbf{G}_1^\dagger(r) - \mathbf{Z}_0\mathbf{G}_2(r) + \frac{i}{2}\mathbf{I}\right]\mathbf{Z}_1 = \mathbf{0}. \tag{3.28}$$

Choosing a starting point $r_c \ll 1$, the solution of the incremental problem can be found by integrating numerically $\mathbf{Z}(r)$ in Equation (3.24) using the initial value $\mathbf{Z}(r_c) = \mathbf{Z}_0 + r_c\mathbf{Z}_1$, with $\mathbf{Z}_0$ and $\mathbf{Z}_1$ given by Equations (3.27) and (3.28), respectively. Performing iterations on all the coefficients determining the order parameter of the bifurcation, the target condition of the numerical integration is given by the boundary condition in Equation (3.7), and reads:

$$\det \mathbf{Z}(r_o) = \mathbf{0}. \tag{3.29}$$

In summary, the elastic boundary problem is transformed into the differential Riccati equation for $\mathbf{Z}$ in Equation (3.24), which can be integrated numerically by imposing the non-singularity of the central-impedance matrix $\mathbf{Z}_0$ and the boundary condition in Equation (3.29). The numerical results are detailed in the next section.

4. Results

In this section, we present results for the linear stability analysis of a soft solid cylinder subjected to finite torsion and axial stretching. We report in turn results for neo-Hookean materials ($c_1 = \mu$, $c_2 = 0$) and for Mooney–Rivlin materials ($c_1 \neq 0$, $c_2 \neq 0$).

As explained in the previous section, the case $m = 1$ requires a special consideration because the matrix $i\mathbf{G}(0)$ then has a doubly degenerate eigenvalue. As a consequence, the central-impedance matrix $\mathbf{Z}_0$ is semi-definite, indicating the occurrence of rigid-body motion modes. As first reported by Green & Spencer (1959) for a neo-Hookean solid, finite non-zero displacements on the axis of the cylinder arise only in the case $m = 1$, leading to the classical problem of a twisted Euler rod, forming an helix of pitch $1/k_z$. This instability can evolve with the sudden onset of a sharply bent ring, or knot (see Fig. 1), as investigated by Gent & Hua (2004). Eventually, the helical patterns can turn into localized writhing in the post-buckling torsional behaviour (Thompson & Champneys, 1996), which can explain, for example, DNA supercoiling (Neukirch & Marko, 2011). Although such effects have been widely investigated in the literature, there seems to be no information to be found regarding higher order torsion instabilities. For this reason, we leave aside the case $m = 1$ in what follows, and we investigate the onset of torsion instabilities with $m \geqslant 2$, corresponding to a zero displacement on the axis of the cylinder.
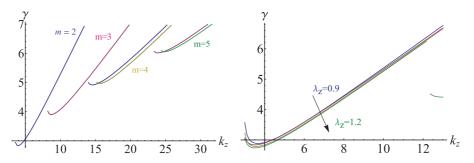
FIG. 4. Instability curves for neo-Hookean materials, showing the critical torsion rate γ versus the longitudinal wavenumber k_z, setting r_o as unit length. The curves are depicted at varying circumferential mode numbers m (left, with $\lambda_z = 1$) and varying axial stretch λ_z (right, with $m = 2$). The axes origin is set at $\gamma = 3$ and $k_z = 5$ for matters of graphical convenience.

4.1 Torsion instabilities for a neo-Hookean material

In the case of a neo-Hookean material (i.e. $c_1 = \mu$, $c_2 = 0$), the Stroh matrix has the simplified form given in Appendix. As first reported by Green & Spencer (1959), the corresponding incremental boundary value problem admits the following analytical solution:

$$U(r) = \sum_{j=1}^{3} A_j \left[I_{m-1}(q_j r) - \frac{m(\lambda_z^{-3} q_j^2 + 2\gamma(m\gamma - k_z) - (\gamma - k_z)^2)}{q_j r (\lambda_z^{-3} q_j^2 - (m\gamma - k_z)^2)} I_m(q_j r) \right],$$

$$V(r) = \frac{1}{r} \sum_{j=1}^{3} A_j \left[\frac{2\gamma r (m\gamma - k_z)}{\lambda_z^{-3} q_j^2 - (m\gamma - k_z)^2} I_{m-1}(q_j r) - \frac{m(\lambda_z^{-3} q_j^2 + 2\gamma(m\gamma - k_z) - (m\gamma - k_z)^2)}{q_j (\lambda_z^{-3} q_j^2 - (m\gamma - k_z)^2)} I_m(q_j r) \right],$$

$$W(r) = \sum_{j=1}^{3} A_j \left[\frac{q_j}{k_z} I_m(q_j r) \right], \tag{4.1}$$

where A_j are arbitrary constants, $I_m(q_j r)$ is the modified Bessel function of the first kind of order m, and $\pm q_j$ are the distinct roots of the following characteristic equation:

$$\lambda_z^{-6} q^6 - \lambda_z^{-3}[\lambda_z^{-3} k_z^2 + 2(m\gamma - k_z)^2]q^4 + (m\gamma - k_z)^2[2\lambda_z^{-3} k_z^2 + (m\gamma - k_z)^2]q^2$$
$$+ k_z^2(m\gamma - k_z)^2[4\gamma^2 - (m\gamma - k_z)^2] = 0. \tag{4.2}$$

However, if the roots of Equation (4.2) are not all distinct (e.g. for $m\gamma = k_z$ there are four roots equal to zero), then the solution in Equation (4.1) is no longer valid. Therefore, the proposed numerical procedure relying on the Riccati equation in Equation (3.24) with Equations (3.27–3.29) is much easier and robust to run to completion in order to derive the instability threshold than by the means of the analytical solution.

Figure 4 depicts our numerical results for the torsion instability of a neo-Hookean material with $m \geqslant 2$, for different circumferential modes numbers m and axial pre-stretches λ_z.

We plot the bifurcation curves with γr_o on the vertical axis and $k_z r_o$ on the horizontal axis. Hence the first quantity is a measure of the angle of torsion, and the second a measure of the cylinder stubbiness R_o/L, according to (3.10). We find that torsion instability occurs with increasing mode numbers m as the stubbiness increases, and that it is slightly promoted by an axial extension of the cylinder (and slightly
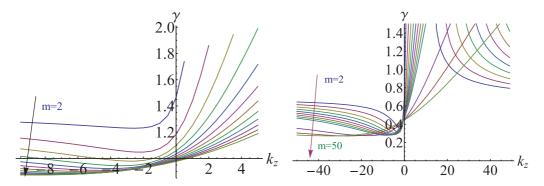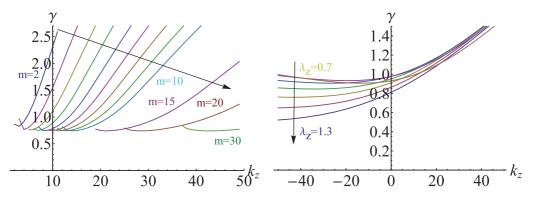
FIG. 5. Instability curves for Mooney–Rivlin materials, showing the critical torsion rate γ versus the longitudinal wavenumber k_z, setting r_o as unit length. The curves are depicted at varying circumferential mode numbers m with $\lambda_z = 1$ for $c_2/c_1 = 1$ (left) and $c_2/c_1 = 1.5$ (right).

FIG. 6. Instability curves for Mooney–Rivlin materials, showing the critical torsion rate γ versus the longitudinal wavenumber k_z, setting R_o as unit length. The curves are depicted at varying circumferential mode numbers m (left, where $c_1 = 0$ and $\lambda_z = 1$) and axial stretch λ_z (right, where $c_2/c_1 = 1$ and $m = 50$).

retarded by axial compression). For instance, in simple torsion, i.e. $\lambda_z = 1$, the earliest critical threshold of torsion instability is found at $m = 2$, $\gamma r_o \simeq 2.83743$, for $k_z r_o \simeq 3.9$.

4.2 *Torsion instabilities for a Mooney–Rivlin material*

In the case of a Mooney–Rivlin material ($c_1 \neq 0$, $c_2 \neq 0$), we find that the onset of the instability is strongly dependent on the value of the ratio of the constitutive parameters c_2/c_1. The results of the incremental boundary value problem are collected in Figs. 5–6.

In particular, we find that the threshold of the torsion rate necessary for the onset of the instability is always lower than for the one found for a neo-Hookean material. Also, both the circumferential and the longitudinal modes of the instability strongly depend on the material constants (e.g. we find $\gamma r_o \simeq 0.2716$, $m = 50$ and $k_z r_o \simeq -43.45$ for $c_2/c_1 = 1.5$ in Fig. 5). Although a general trend cannot be clearly identified, it seems that a surface instability mechanism at high mode number m is the dominant scenario for Mooney–Rivlin materials.

5. Discussion and conclusions

We investigated the occurrence of elastic instabilities of a soft incompressible cylinder subjected to a combination of finite axial stretching and finite torsion. We assumed a Mooney–Rivlin constitutive relation in Equation (2.3) in order to account for weakly nonlinear effects up to third order in the strain. The basic axial-symmetric deformation is given by Equation (2.1), and the elastic solution for the normal force and the torque at the top surfaces is given by Equations (2.12) and (2.13). Using the theory of incremental elastic deformations superimposed on finite strains, we derived the Stroh formulation of the incremental boundary elastic problem in Equation (3.15). Introducing the surface impedance matrix $\mathbf{Z}$ in Equation (3.23), we rewrote the differential system as a differential Riccati equation in Equation (3.24). In this theoretical framework, the central-impedance matrix $\mathbf{Z}_0$ plays a fundamental role for determining the incremental solution. In order to define a robust numerical procedure, we identified such a matrix as the stable solution of the algebraic Riccati equation in Equation (3.27), hence avoiding singularities at $r = 0$. Finally, we computed the numerical solutions by performing iterations on the order parameters driving the elastic bifurcation, while the onset of the instability is given by the target condition of Equation (3.29).

Leaving aside the oft-studied case of twisting instability, see Fig. 1, we focused instead on the occurrence of torsion instability, i.e. the formation of surface wrinkles occurring when the axis displacements are prevented by geometrical constraints, see Fig. 2. In the case of a neo-Hookean material, the marginal stability curves are depicted in Fig. 4. The critical threshold for the torsion rate in the case of simple torsion is calculated for $\gamma r_o \simeq 2.83743$, within the experimental range found by Mora *et al.* (2011). The marginal stability curves for a Mooney–Rivlin material are depicted in Figs. 5–6 for different ratios c_2/c_1 of elastic coefficients and axial pre-stretch λ_z. In particular, we find that a surface instability mechanism arises, i.e. formation of wrinkles with short circumferential and axial wavelengths, with lower values of the critical threshold for the torsion rate.

In conclusion, we demonstrated that a subclass of torsional instabilities occur when the axis displacement of the cylinder is prevented. The validity of our new theoretical predictions could be easily checked experimentally by applying finite torsion and axial stretch with a rheometer to a soft, incompressible cylinder having a small axial length/external diameter ratio.

REFERENCES

DE PASCALIS, R., DESTRADE, M. & GORIELY, A. (2011) Nonlinear correction to the Euler buckling formula for compressed cylinders with guided-guided end conditions. *J. Elasticity,* **102**, 191–200.

DESTRADE, M., GILCHRIST, M. D., & MURPHY, J. G. (2010) Onset of non-linearity in the elastic bending of blocks. *ASME J. Appl. Mech.*, **77**, 061015.

DROZDOV, A. D. (1996) *Finite Elasticity and Viscoelasticity: A Course in the Nonlinear Mechanics of Solids*. World Scientific.

DUKA, E. D., ENGLAND, A. H. & SPENCER, A. J. M. (1993) Bifurcation of a solid circular cylinder under finite extension and torsion. *Acta Mech.*, **98**, 107–121.

GENT, A. N. & HUA, K.-C. (2004). Torsional instability of stretched rubber cylinders. *Int. J. Nonlin. Mech.*, **39**, 433–439.

GREEN, A. E. & SPENCER, A. J. M. (1959). The stability of a circular cylinder under finite extension and torsion. *J. Math. Phys*, **37**, 316–338.

HORGAN, C. O. & SACCOMANDI, G. (1999) Simple torsion of isotropic, hyperelastic, incompressible materials with limitingchain extensibility. *J. Elasticity*, **56**, 159–170.

MORA, S., ABKARIAN, M., TABUTEAU, H. & POMEAU, Y. (2011) Surface instability of soft solids under strain. *Soft Matter*, **7**, 10612–10619.

NEUKIRCH, S. & MARKO, J. F. (2011). Analytical description of extension, torque, and supercoiling radius of a stretched twisted DNA. *Phys. Rev. Lett.*, **106**, 138104.

NORRIS, A. N. & SHUVALOV, A. L. (2010). Wave impedance matrices for cylindrically anisotropic radially inhomogeneous elastic solids. *Q. Jl Mech. Appl. Math.*, **63**, 401–435.

OGDEN, R. W. (1997) *Nonlinear Elastic Deformations*. New York: Dover.

POYNTING, J. H. (1909) The wave motion of a revolving shaft, and a suggestion as to the angular momentum in a beam of circularly polarised light. *Phil. Trans. R. Soc. Lond. A*, **82**, 560–567.

RIVLIN, R. S. (1948a) Large elastic deformations of isotropic materials. III. Some simple problems in cylindrical polar co-ordinates. *Phil. Trans. R. Soc. Lond. A*, **240**, 509–525.

RIVLIN, R. S. (1948b) Large elastic deformations of isotropic materials. IV Further developments of the general theory. *Phil. Trans. R. Soc. Lond. A*, **241**, 379–397.

RIVLIN, R. S. (1949) Large elastic deformations of isotropic materials. VI. Further results in the theory of torsion, shear and flexure. *Phil. Trans. R. Soc. Lond. A*, **242**, 173–195.

RIVLIN, R. S. & SAUNDERS, D. W. (1951). Large elastic deformations of isotropic materials. VII. Experiments on the deformation of rubber. *Phil. Trans. R. Soc. Lond. A*, **243**, 251–288.

SHUVALOV, A. L. (2003). The Frobenius power series solution for cylindrically anisotropic radially inhomogeneous elastic materials. *Q. Jl Mech. Appl. Math.*, **56**, 327–345.

THOMPSON, J. M. T. & CHAMPNEYS, A. R. (1996). From helix to localized writhing in the torsional post-buckling of elastic rods. *Proc. R. Soc. A*, **452**, 117–138.

WINEMAN, A. (2004). Some results for generalized neo-Hookean elastic materials. *Int. J. Nonlin. Mech.*, **40**, 271–279.

Appendix. Stroh matrix for a neo-Hookean material

Let us consider a neo-Hookean material, setting $c_1 = \mu$ and $c_2 = 0$ in Equation (2.3). In this case, from Equations (3.4) the instantaneous elastic moduli reduce to

$$L_{jilk} = \mu b_{jl}\delta_{ik}. \tag{A.1}$$

Substituting Equations (2.4) and (A.1) into Equation (3.15), the blocks of the Stroh matrix take the following forms:

$$\mathbf{G}_1 = \begin{bmatrix} i & im & -ik_z r \\ -\frac{1}{2}im\left[2 + \gamma^2\lambda_z^2\left(R_o^2 - r^2\lambda_z\right)\right] & -\frac{1}{2}i\left[2 + \gamma^2\lambda_z^2\left(R_o^2 - r^2\lambda_z\right)\right] & 0 \\ \frac{1}{2}ik_z r\left[2 + \gamma^2\lambda_z^2\left(R_o^2 - r^2\lambda_z\right)\right] & 0 & 0 \end{bmatrix} \tag{A.2}$$

and

$$\mathbf{G}_2 = \begin{bmatrix} 0 & 0 & 0 \\ 0 & -\lambda_z/\mu & 0 \\ 0 & 0 & -\lambda_z/\mu \end{bmatrix}, \quad \mathbf{G}_3 = \begin{bmatrix} -\dfrac{\alpha_1\mu}{4\lambda_z} & -\dfrac{\alpha_{12}\mu}{4\lambda_z} & -\dfrac{\alpha_{13}\mu}{2\lambda_z} \\[2mm] -\dfrac{\alpha_{12}\mu}{4\lambda_z} & -\dfrac{\alpha_2\mu}{4\lambda_z} & -\dfrac{\alpha_{23}\mu}{\lambda_z} \\[2mm] -\dfrac{\alpha_{13}\mu}{2\lambda_z} & -\dfrac{\alpha_{23}\mu}{\lambda_z} & \dfrac{\alpha_3\mu}{\lambda_z} \end{bmatrix} \tag{A.3}$$

with

$$\begin{cases} \alpha_1 = (-16 + 8\gamma k_z m r^2 \lambda_z^3 + \gamma^4\, m^2 \lambda_z^4 (R_o^2 - r^2\lambda_z)^2 - 4\gamma^2\lambda_z^2(R_o^2 - m^2 R_o^2 + 2m^2 r^2 \lambda_z) \\ \qquad + k_z^2 r^2 (4 + \lambda_z^2(-4\lambda_z + \gamma^2(R_o^2 - r^2\lambda_z)(4 + \gamma^2\lambda_z^2(R_o^2 - r^2\lambda_z)))))), \\ \alpha_2 = (8\gamma k_z m r^2 \lambda_z^3 - 4\,m^2(4 + \gamma^2 R_o^2\lambda_z^2) + \lambda_z^2(-4k_z^2 r^2\lambda_z + 4\gamma^2(R_o^2 - 2r^2\lambda_z) + \gamma^4\lambda_z^2(R_o^2 - r^2\lambda_z)^2)), \\ \alpha_3 = (m^2 + \gamma r^2(-2k_z m + \gamma m^2 - \gamma k_z^2 r^2)\lambda_z^3 + k_z^2 r^2(3 + \gamma^2 R_o^2\lambda_z^2 + \lambda_z^3)), \\ \alpha_{12} = (8\gamma k_z r^2 \lambda_z^3 + m(-16 - 8\gamma^2 r^2\lambda_z^3 + \gamma^4\lambda_z^4(R_o^2 - r^2\lambda_z)^2)), \\ \alpha_{13} = k_z r(4 + \gamma^2\lambda_z^2(R_o^2 - r^2\lambda_z)), \\ \alpha_{23} = k_z m r(3 + \gamma^2\lambda_z^2(R_o^2 - r^2\lambda_z)). \end{cases}$$

$$\tag{A.4}$$